MODELING OF SECONDARY MOTIONS DRIVEN BY THE TURBULENCE ANISOTROPY IN CLOSED AND OPEN CHANNELS

Amel Soualmia, Sahbi Zaouali and Chouaib Labiod [1]

Ecole Nationale d'Ingénieurs de Tunis, LMHE, B.P. 37 Le Belvédère, 1002 Tunis, Tunisie
[1] Université de Jijel, Laboratoire de Génie Géologique, B.P. 98, Ouled Aissa, 18000 Jijel, Algérie
amel.soualmia@ipeim.rnu.tn

ABSTRACT

The capabilities of Reynolds stress models to predict the hydrodynamic response of open channel turbulent flows to fixed bed roughness heterogeneity are analyzed. An algebraic model is used, issued from the Reynolds stress transport model of Gibson and Launder (1978), adapted by Gibson and Rodi (1989) to simulate the effects of the wall and the free surface on the turbulence anisotropy. This model is first tested in parallel free surface flows with smooth or rough bottom. Then, it is applied to non-parallel closed or open channel flows with different configurations of the wall roughness for which experimental results are available.

INTRODUCTION

Turbulent free surface flows, in urbanized or natural media, frequently occur with inhomogeneous boundary conditions due to roughness variations of fixed or mobile beds. These flows present complexities that often constitute limitations of existing models: this is the case for 3D models, founded on one point turbulence closures, as well as for 1D or 2D Saint-Venant models, obtained by section or vertical integration and used currently in field applications. The calculation of such flows requires second-order closure models of the Reynolds stresses allowing an accurate prediction of the turbulence anisotropy that controls the generation of secondary flows. Since the first works on Reynolds-stress closures of Launder, Reece and Rodi (1975), Zeman and Lumley (1976), Gibson and Launder (1978), some authors, like Gessner and Emery (1981), Demuren and Rodi (1984), Celik and Rodi (1984), Gibson and Rodi (1989), Launder and Li (1994), Naimi and Gessner (1997), Spezial, Sarkar and Gatski (1991), Cokljat and Younis (1995) proposed improvements of second order turbulence models to predict secondary flows in non circular channels. Despite these works, many difficulties remain due notably to the effects of large roughness on the turbulence anisotropy in the wall region and near the free surface.

In the present work, the capabilities of algebraic stress models are analyzed to predict the hydrodynamic response of turbulent open channel flows to fixed bed roughness heterogeneity. The model is tested first in parallel free surface flows and then in non-parallel closed or open channel flows.

PRESENTATION OF THE ALGEBRAIC MODEL

Mean flow equations

Fully developed flows are considered in straight, rectangular, closed or open channel flow with constant bed slope α. In the following, x, y, and z are the longitudinal, transverse and nearly vertical coordinates; U,V,W and u, v, w are the (x, y, z)-components of the ensemble mean velocity U_i and the velocity fluctuations u_i respectively. The equations of the mean motion may be written in the following form, where the equations of secondary flow are expressed in terms of the vorticity Ω and the stream function ψ of secondary motions (V, W):

$$V\frac{\partial U}{\partial y} + W\frac{\partial U}{\partial z} = \frac{\partial}{\partial z}(-\overline{uw}) + \frac{\partial}{\partial y}(-\overline{uv}) - \frac{1}{\rho}\frac{dp}{dx} - g\sin\alpha \tag{1}$$

$$V\frac{\partial \Omega}{\partial y} + W\frac{\partial \Omega}{\partial z} = -\frac{\partial^2}{\partial y \partial z}(\overline{w^2} - \overline{v^2}) - \left(\frac{\partial^2}{\partial z^2} - \frac{\partial^2}{\partial y^2}\right)(\overline{vw}) \tag{2}$$

$$\nabla^2 \Psi = -\Omega \tag{3-a}$$

Where $\quad V = \dfrac{\partial \Psi}{\partial z} \quad , \quad W = -\dfrac{\partial \Psi}{\partial y}$ \hfill (3-b)

In equations (1) to (3) the fluid viscosity was ignored as a consequence of developed turbulence assumption.

The algebraic Reynolds stress model

The algebraic model of Reynolds stress tensor, $\overline{u_i u_j}$ used in this work is issued from the Reynolds stress transport model of Gibson & Launder (1978). It may be expressed as:

$$2(C_1 + \frac{P}{\varepsilon} - 1)b_{ij} = (1 - C_2)\frac{\pi_{ij}}{\varepsilon} + \left[G_{ij}(b_{km}, n_i) + H_{ij}(\frac{\pi_{ij}}{\varepsilon}, n_i) \right] f_S(\frac{L}{n_i r_i}) \tag{4}$$

Where ε is the dissipation rate of the turbulent kinetic energy $k = \overline{u_j u_j}/2$ (TKE). The anisotropy tensor b_{ij} is defined as $b_{ij} = (\overline{u_i u_j} - \frac{2k}{3}\delta_{ij})/2k$ and π_{ij} is the deviator of the production rate tensor $P_{ij} = -\overline{u_i u_k}\frac{\partial U_j}{\partial x_k} - \overline{u_j u_k}\frac{\partial U_i}{\partial x_k}$; $P = 0.5P_{ii}$ is the production rate

of TKE, C_1 and C_2 are constants. The second term on the right of Eq. (4) represents the damping effects of boundary surfaces on turbulent stresses: $f_S(\dfrac{L}{n_i r_i})$ is a surface (wall or free surface) proximity function, where n is the unit vector normal to the surface; r is the position vector and the characteristic turbulent length scale L is defined as $L = k^{3/2}/\varepsilon$. The tensors G_{ij} and H_{ij} are expressed following the formulation of Shir (1973).

This model is applied to fully developed flow by introducing some simplifications. And so, the Reynolds tensor normal components $\overline{v^2}$ and $\overline{w^2}$ that drive secondary motion vorticity may be written in the following form:

$$\overline{w^2} = \frac{k(G_w + c_1' \dfrac{\overline{v^2}}{k} f_{wl})}{C_1 + \dfrac{P}{\varepsilon} - 1 + 2c_1' f} - 2\nu_t \frac{\partial W}{\partial z} \tag{5-a}$$

Where: $G_w = \dfrac{2}{3}(C_1 - 1) + \dfrac{2}{3} C_2 \dfrac{P}{\varepsilon}(1 + c_2'(f_{wl} - 2f))$ (5-b)

$$\overline{v^2} = \frac{k(G_v + c_1' \dfrac{\overline{w^2}}{k} f)}{C_1 + \dfrac{P}{\varepsilon} - 1 + 2c_1' f_{wl}} - 2\nu_t \frac{\partial V}{\partial y} \tag{6-a}$$

Where: $G_v = \dfrac{2}{3}(C_1 - 1) + \dfrac{2}{3} C_2 \dfrac{P}{\varepsilon}(1 + c_2'(f - 2f_{wl}))$ (6-b)

The first simplification of the Gibson & Launder (1978) model, concerns the last terms in the right-hand side of equations (5) and (6): in fact, the terms $-2\nu_t \partial W/\partial z$ and $-2\nu_t \partial V/\partial y$ regroup the contributions of secondary velocity gradients as proposed by Naot and Rodi (1982), (these are neglected in most other models); the turbulent viscosity being given by the standard expression:

$$\nu_t = C_\mu k^2/\varepsilon \quad \text{in which } C_\mu = \text{Constant} \tag{7}$$

In equations (5) to (6), the surface function f regroups the damping effects due to the channel bottom and the free surface (in open channel flows) as $f = f_{wb} + f_{fs}$. For f_{wb} and f_{fs} the formulation of Gibson and Rodi (1989) was taken up:

$$f_{wb} = \frac{L}{ah} \xi^{-1} (1 - \xi)^2 \quad \text{and} \quad f_{fs} = \frac{L}{ah} \xi^2 (1 - \xi)^{-1} \tag{8}$$

h is the half-height of the rectangular closed channel or the water depth of the open channel; $\xi = z/h$ is the non-dimensional vertical coordinate and a is a constant. The surface function

f_{wl} that represents the damping effect of the lateral walls was expressed in a form similar to (8) in terms of the non-dimensional coordinate $\zeta = y/b$ where b is the half-width of the channel.

$$f_{wl} = \frac{L}{ah} g(\zeta, h/b) \qquad (9\text{-a})$$

Where the function g was given by:

if $\quad 0 \le \zeta \le 1 - h/b, \; g = 0$

if $\quad 1 - h/b \le \zeta \le 1, \; g = \frac{b}{h} \frac{(1 - h/b - \zeta)^2}{(1 - \zeta)} \qquad (9\text{-b})$

The second simplification of the generic model concerns the expressions of the turbulent shear stresses, expressed as:

$$-\overline{uw} = \nu_t \frac{\partial U}{\partial z} \qquad\qquad -\overline{uv} = \nu_t \frac{\partial U}{\partial y} \qquad (10)$$

$$-\overline{vw} = \nu_t \left(\frac{\partial V}{\partial z} + \frac{\partial W}{\partial y} \right) \qquad (11)$$

The turbulent viscosity is given by (7) and the simplification consists to assume a constant value of the diffusion parameter C_μ instead of its functional expressions in the generic model (Zaouali, 2008; Zaouali *et al.*, 2007). In fact, this would make the calculation more rapid. Because a refined turbulence model is not so essential for calculating the primary shear stresses, the approach of existing models is so adopted to determine these stresses with the aid of the isotropic eddy – viscosity hypothesis.

The Reynolds stress model (5) to (11) was completed by transport equation of the TKE and the dissipation rate:

$$V \frac{\partial k}{\partial y} + W \frac{\partial k}{\partial z} = \frac{\partial}{\partial y}(c_k \frac{\overline{v^2}}{k} \frac{k^2}{\varepsilon} \frac{\partial k}{\partial y}) + \frac{\partial}{\partial z}(c_k \frac{\overline{w^2}}{k} \frac{k^2}{\varepsilon} \frac{\partial k}{\partial z}) + P - \varepsilon \qquad (12)$$

$$V \frac{\partial \varepsilon}{\partial y} + W \frac{\partial \varepsilon}{\partial z} = \frac{\partial}{\partial y}(c_\varepsilon \frac{\overline{v^2}}{k} \frac{k^2}{\varepsilon} \frac{\partial \varepsilon}{\partial y}) + \frac{\partial}{\partial z}(c_\varepsilon \frac{\overline{w^2}}{k} \frac{k^2}{\varepsilon} \frac{\partial \varepsilon}{\partial z}) + P_\varepsilon - C_{\varepsilon 2} \frac{\varepsilon^2}{k} \qquad (13)$$

The dissipation production rate in the equation (13) was modeled following the standard formulation:

$$P_\varepsilon = C_{\varepsilon 1} \frac{\varepsilon}{k} P \qquad (14\text{-a})$$

or following the alternative formulation of Zeman and Lumley (1976):

$$P_\varepsilon = 0.47 \frac{\varepsilon}{k} P + 3.9 \frac{\varepsilon^2}{k} \frac{b_{ij} b_{ij}}{1 + 1.5 \sqrt{b_{ij} b_{ij}}} \qquad (14\text{-b})$$

Boundary conditions

At the walls, (bottom or lateral wall), the standard boundary conditions are applied for the longitudinal velocity and for the TKE and the dissipation rate at a distance d_n from the wall where the turbulence is developed:

$$U / u^* = \kappa^{-1} Ln \left[d_n / K_s (1 + \frac{3.32\nu}{u^* K_s}) \right] + 8.5 \qquad (15\text{-}a)$$

$$k = C_{\mu z}^{-0.5} u^{*2} , \; \varepsilon = u^{*3} / \kappa d_n \qquad (15\text{-}b)$$

The equation (15-a), where K_s is the roughness height, is valid for smooth, rough and intermediate regime. The wall boundary conditions for the stream function and the vorticity of the secondary flows, at the distance d_n, are:

$$\psi = 0 , \; \Omega = 0 \qquad (15\text{-}c)$$

At the symmetry axis of closed channel or at the free surface of open channel (z=h), the following boundary conditions were applied:

$$z = h, \frac{\partial U}{\partial y} = \frac{\partial k}{\partial y} = \frac{\partial \varepsilon}{\partial y} = 0, \Psi = \Omega = 0 \qquad (16\text{-}a)$$

In the case of open channel flow it was observed that the boundary condition proposed by Naot and Rodi (1982) for the dissipation rate gives better results and so:

$$z = h, \varepsilon = \kappa^{-1} C_\mu^{3/4} k_s^{3/2} (\frac{1}{0.2h} + \frac{1}{y^*}) \qquad (16\text{-}b)$$

Where y * is the distance to the lateral wall.

Numerical resolution

Concerning the numerical resolution, because of symmetrical conditions (for the following application cases), the resolution is considered only on the half cross section of the channels. A uniformly distributed grid (leading to square cells) is used for the finite volume method employed. Test calculations were also carried out with tighter grid for each case, they yielded secondary velocities which differed by less than 5% from those obtained with the used coarser grid. The system was resolved by Stone's iterative method, and the convergence was obtained after about thousand iterations.

RESULTS AND DISCUSSIONS

Application to parallel flow over smooth and rough wall in closed and open channel

This model is first applied to simulate parallel, fully developed closed channel flows, and comparing them to result experiments of Comte-Bellot (1965) and Clark (1968).

These experiments were achieved in channels of large shape ratio; the values of the Reynolds numbers, based on the maximum velocity, are Re = 4.56 x 10^4 and Re = 5.7 x 10^4; in the two experiments the ratio of the friction velocity to the maximum velocity is the same, $u^*/U_{max} = 0.037$. In Fig.1, the profiles of longitudinal and vertical fluctuations, $\overline{u^2}$ and $\overline{w^2}$, are plotted, normalized by the friction velocity u* in terms of $\xi = z/h$. The curves (pointed as Sim) represent the results of numerical simulations obtained with the turbulence model defined by equations (5) to (14), but with parallel flow assumption (V=W=0), and with the values of the constants indicated in Table 1.

TABLE 1

Values of the Model Constants

C_1	C_2	c_1'	c_2'	a	$C_{\varepsilon 1}$	$C_{\varepsilon 2}$	c_k	c_ε
1.8	0.6	0.5	0.3	3.18	1.44	1.92	0.22	0.18

-In the wall region ($\xi < 0.2$), the component $\overline{u^2}/u^{*2}$ is slightly underpredicted. For the vertical component, in this zone, the simulations seem to reproduce better Comte Bellot results.

-Out of this zone, the simulations reproduce acceptably the experimental results of the longitudinal component $\overline{u^2}/u^{*2}$ (Fig. 1a). It is also noted that for the vertical component the simulations join Comte-Bellot (1965) experiments (Fig. 1b).

These simulations were obtained with $C_\mu = 0.05$.
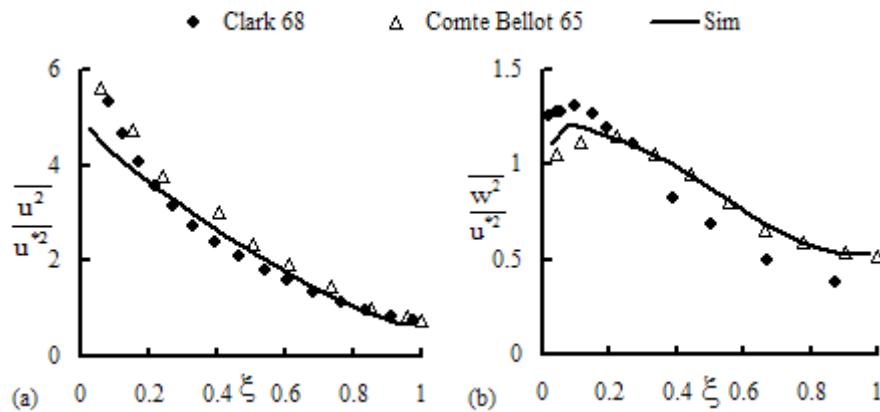
Figure 1. Longitudinal (a) and vertical (b) velocity fluctuations in closed channel flow.

Secondly this model is applied to simulate also parallel fully developed flows, but in open channels over smooth bed (it's the experiments pointed out as runs P3 and P4 in Nezu and Rodi (1986), and over rough bed (it's the run E0 in Labiod and Masbernat (2004)). These experiments were achieved in channels of large shape ratio (2b/h>5) and the mean velocity and Reynolds tensor components profiles measured in the center of the channel were not affected by secondary flows; so the model was applied here too with parallel flow assumption (V=W=0). The normal components of the Reynolds tensor are plotted on Figure 2.
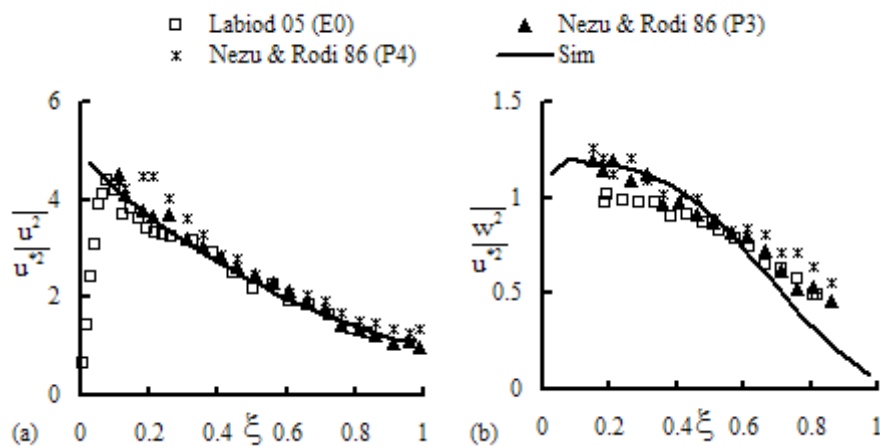
Figure 2. Longitudinal (a) and vertical (b) velocity fluctuations in open channel flow.

It is shown that these profiles of $\overline{u^2}/u^{*2}$ and $\overline{w^2}/u^{*2}$ obtained with $C_\mu = 0.05$ are satisfactory predicted. In fact, it is observed that this algebraic model predicts relatively well the increase and the diminution of these normal velocity fluctuations near the wall and near the free surface.

Then this model is used to simulate non-parallel, fully developed flows in closed and open channel flows with different configurations of wall roughness.

Application to square closed and open smooth channel

Simulations of the flow in square corner are achieved and are compared with experimental results obtained:
- In square closed channels, by Nezu and Nakagawa (1984), Lund (1977), Donald *et al*. (1984), Eppich (1982).
- In open channels, by Nezu and Rodi (1985).

        In Figures 3 and 4 the secondary flow field is compared in closed and open channel respectively. A good agreement is observed between experimental and theoretical results with an important difference between closed and open channel due to the damping effect of the free surface (as shown by the anisotropy profile in Fig. 5). In fact secondary flow patterns in ducts are symmetrical with regard to the corner bisector (Fig. 3), while those in open channels are not (Fig. 4). In the free – surface region a large cell appears, from the side wall toward the channel centre, and the down – flow along the channel centre from the free surface toward the bed, this is peculiar to open channel flows, as indicated by others.

        In Fig. 5, the simulation results of Demuren and Rodi (1984) achieved with a Reynolds stress transport model were also plotted.
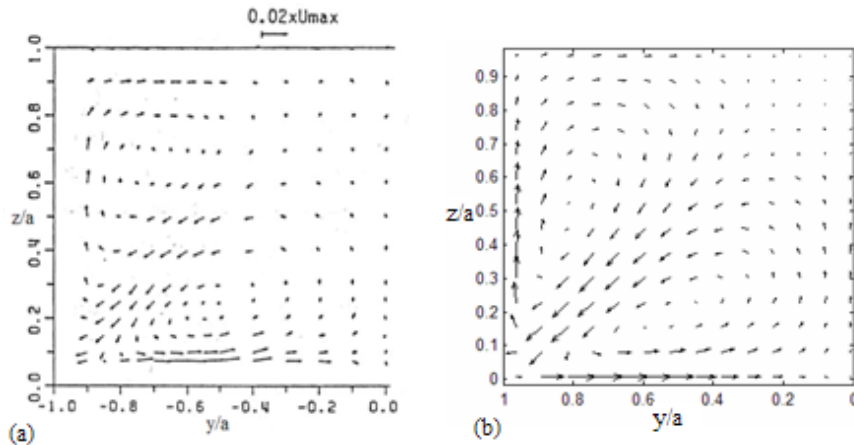

Figure 3. Secondary flow velocity in closed duct:
(a)   measured by Nezu and Nakagawa (1984); (b) present prediction.
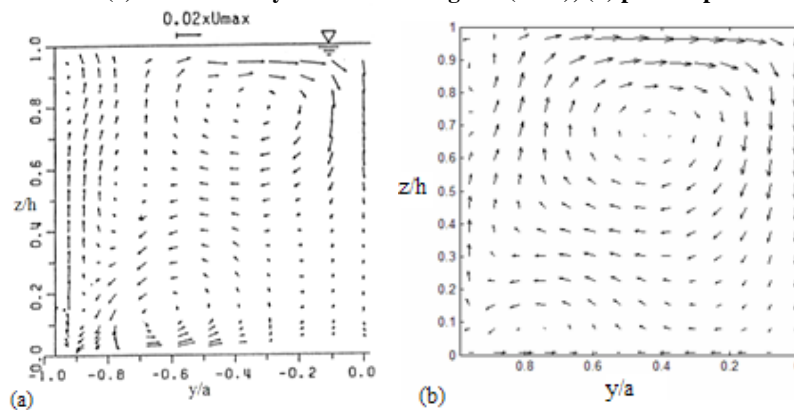
Figure 4. Secondary-current in open channel:
(a) measured by Nezu and Rodi (1985); (b) present prediction.

In Fig. 6, it can be observed that the prediction of the wall shear stress is satisfactory for both closed and open channel.

The longitudinal velocity profiles, normalised by the mean velocity plotted on Figure 7a show the simulations over predict slightly the velocity on the wall region. This agrees with the undervaluation of the wall friction in this zone (Fig. 6). While the vertical velocity component, normalised by the mean wall friction velocity (Fig. 7b), confirms these observations concerning the capability of this model to reproduce the secondary flow intensities. It is noted that the simulations results here coincide better with Brundett and Baines (1964) measurements.
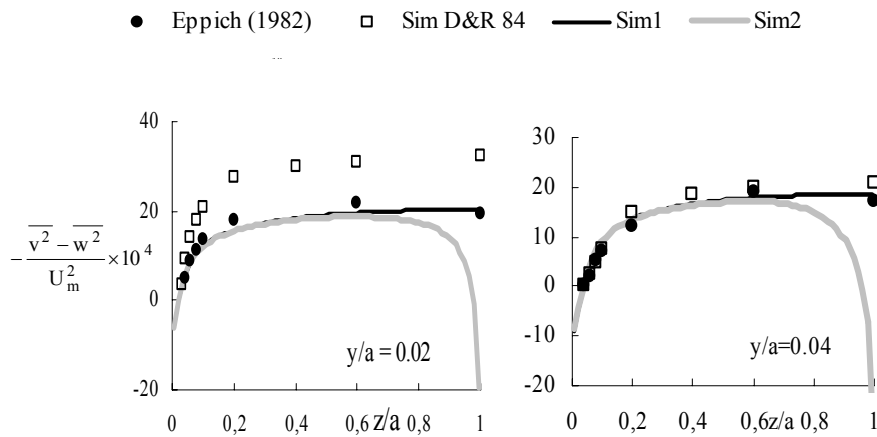
**Figure 5. Turbulence anisotropy in closed square duct (sim1)
and open channel with 2B/h=2 (sim2).**

Application to Hinze experiment (1973)

In this experiment achieved in a partially rough duct, Hinze measured the axial mean velocity field (Fig. 8), and the profiles, on the centreline of the duct, of the Reynolds shear stress (Fig. 10), and the vertical component of secondary flow (Fig. 9). It is noted that this simplified model gives as good a result as the more sophisticated models of Launder and Li (1994) or Naimi and Gessner (1997).

In Figure 11, are presented the secondary flow patterns obtained from simulations of Muller and Studerus (1979) Experiment, achieved with the algebraic Reynolds stress model. Secondary flows are organized in two counter-rotating cells, oriented, near the wall, from the

rough strip towards the smooth strip, and their main characteristics are near to the experimental results.
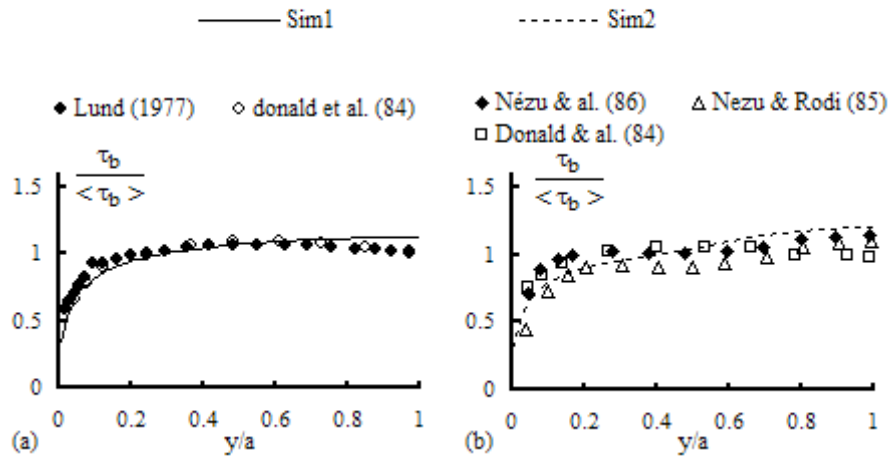

**Figure 6. Distribution of bed shear stress τ_b for closed square duct (sim1)
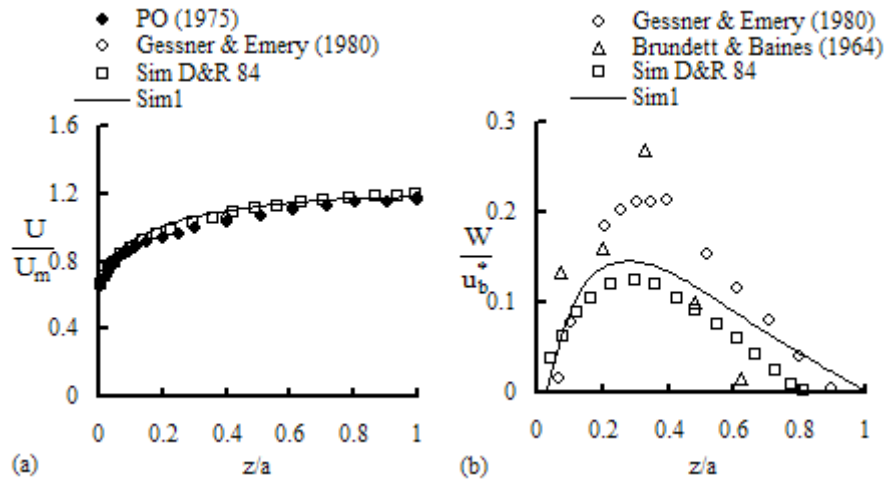and open channel with 2B/h=2 (sim2).**

**Figure 7. Vertical profiles: (a) longitudinal velocity on the duct midline;
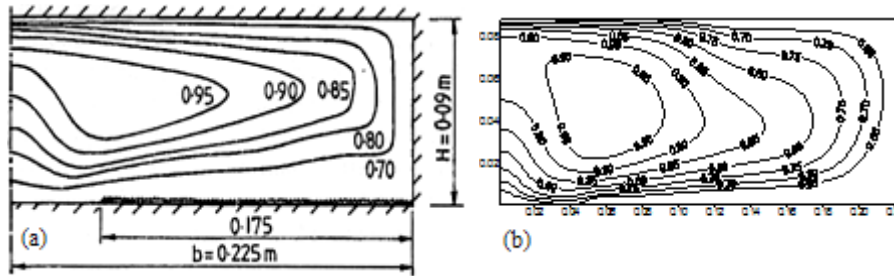(b) Secondary flow velocity near the lateral wall.**

Figure 8. Isovelocity streamlines in a partially rough duct; (a) Hinze's experiment; (b) present simulation.
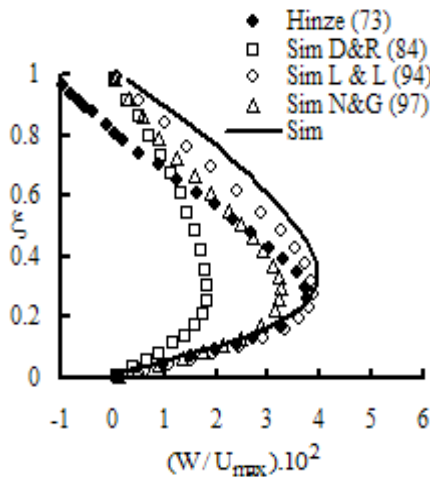

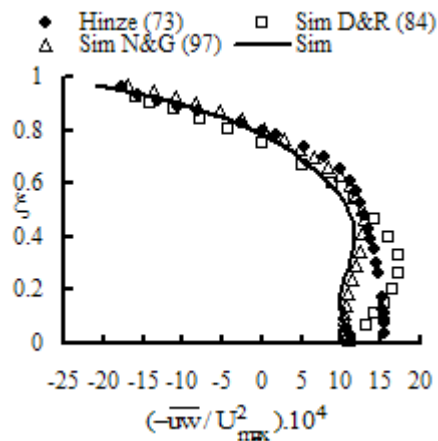| **Figure 9. Secondary flow velocity profiles on the duct midline.** | **Figure 10. Turbulence shear stress profiles on the duct midline.** |

Application to experiments of Muller & Studerus (1979), and Wang and Cheng (2006) in rectangular open channel, over smooth and rough bed strips

In fact the maximum magnitude of the secondary velocity vectors is about 0.02 Um. On Figure 12, the effect of the sharp roughness change on the distribution of τ_b was observed; a good agreement with Muller experiment for τ_b measurements are available.
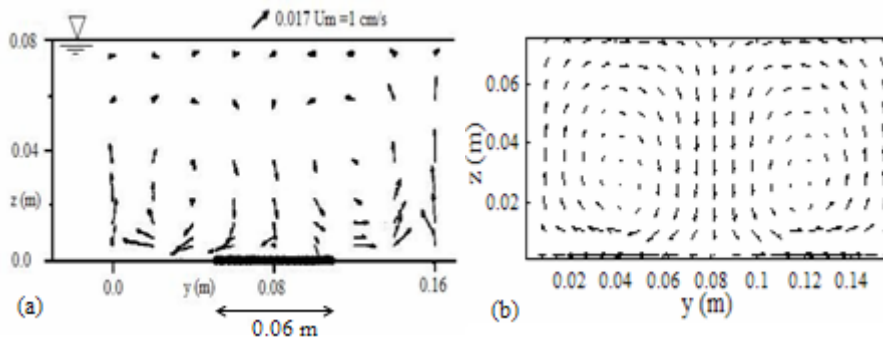
Figure 11. Secondary-current velocity vector over smooth and rough bed strips in rectangular open channel; (a) Muller and Studerus (1979); (b) present prediction.
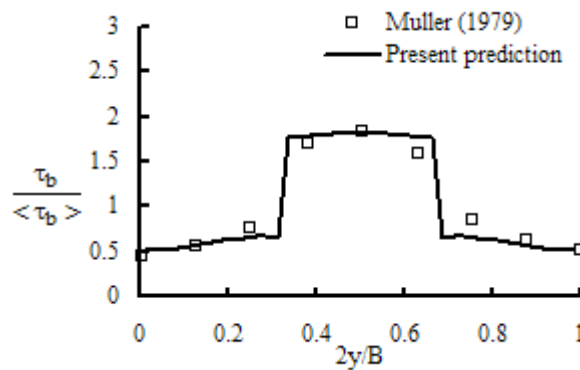

Figure 12. Distribution of bed shear stress τ over smooth and rough bed strips in rectangular open channel.

On Figure 13b, the vertical profiles of the vertical velocity │W│/Um are reported . It is observed that the simulations give intensities of │W│/Um that are close at the verticals y = 0, 16 and 8 (Fig. 13b); while the measurements show profiles with higher intensities over rough zone (y = 8), than over smooth zone (y = 0 and 16). On Figure 13 a, the vertical simulated and measured profiles of the longitudinal velocity component are also compared . It is observed that the simulations reproduce the transversal velocity distribution, characterised by a more important mass flow rate in the channel center (rough zone), than over smooth zones.
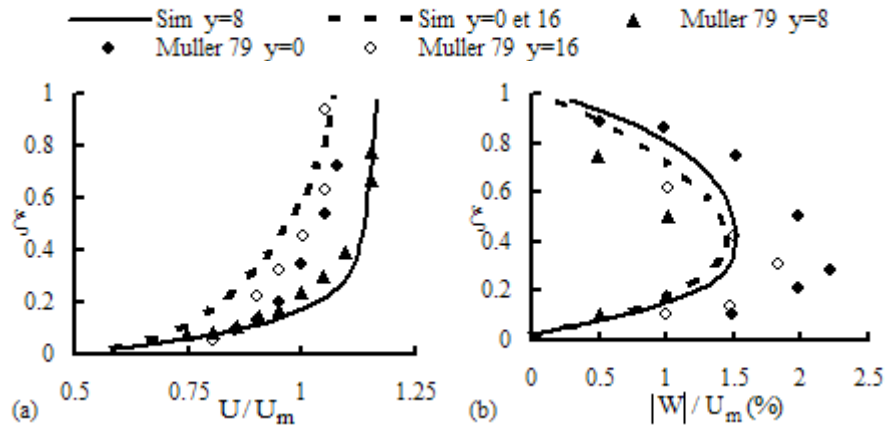
Figure 13. Vertical profiles (a) longitudinal velocity; (b) Secondary flow velocity (Experiments of Muller and Studerus (1979)).

The simulations of Wang and Cheng (2006) experiment reported on Figure 14 confirmed the previous observations: well reproduction of the cellular organisation of the secondary flows, which are oriented from the rough zone towards the smooth one (Fig. 14a); and well prediction of the secondary flows intensity (the maximum magnitude of the secondary velocity vectors is about 0.025 Um).

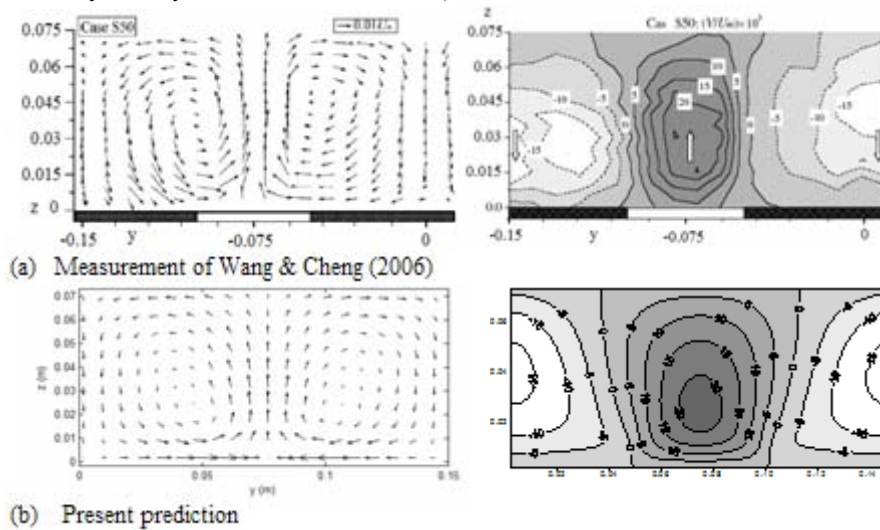(a) Measurement of Wang & Cheng (2006)

(b) Present prediction

Figure 14. Secondary-current velocity vector and isovelocity streamlines of the vertical component: (a) measurement of Wang and Cheng (2006); (b) present prediction.

CONCLUSION

In this study an algebraic stress model was applied to a variety of available laboratory experiments existing in literature. The analysis shows that this model allows to predict correctly the vertical profiles of the Reynolds stress tensor components, the local bottom friction, the primary isovelocity, and the secondary flow velocity. It is noted in particular that close to the wall, in the zone of roughness change (for the rough walls), the model confirms the role of the secondary flows on the turbulence intensity *via* the decrease of the turbulence production due to the decrease of the shear stress. It has to be noted that the model was applied only to laboratory experiments, and it will be interesting to test it for real cases. In prospect the simulation results of this model could be used to analyze the closure problem of Saint-Venant model, that is more adequate for the prediction of the flows in environmental situations; and then other experimental results will be tested to generalize and improve analisis of scale change problems in complex flows.

REFERENCES

Celik, I. and Rodi, W. 1984. Simulation of free-surface effects in turbulent channel flows. *PCH Physico Chemical Hydrodynamics*, 5(3/4): 217-227.

Clark, J. A. 1968. A study of incompressible turbulent boundary layers in channel flow. *J. Basic Eng., ASME.*, 90: 455-468.

Cokljat, D. and Younis, B.A. 1995. Second-order closure study of open-channel flows. *Journal of Hydraulics Engineering, ASME,* 121: 94-107.

Comte-Bellot, G. 1965. *Ecoulement turbulent entre deux parois parallèles.* Publications scientifiques et techniques du Ministère de l'air, no. 419.

Demuren, A. and Rodi, W. 1984. Calculation of turbulence-driven secondary motion in non-circular ducts. *Journal of Fluid Mechanics*, 140: 189-222.

Donald, K., John, D. and Mohammed, H. 1984. Boundary shear in smooth rectangular channels. *Journal of Hydraulic Engineering, ASCE*, 110 (4): 405-422.

Eppich, H.M. 1982. *The development and preliminary testing of a constitutive model for turbulent flow along a streamwise corner*, PhD.

Gessner, F.B. and Emery, A.F. 1981. The numerical prediction of Developing turbulent flow in rectangular ducts. *Journal of Fluid Engineering*, *ASME,* 103: 445-454.

Gibson, M.M. and Launder, B.E. 1978. Grounds effects on pressure fluctuations in the atmospheric boundary layer. *Journal of Fluid Mechanics*, 86: 491-511.

Gibson, M.M. and Rodi, W. 1989. Simulation of free surface effects on turbulence with a Reynolds stress model. *Journal of Hydraulic Research,* 27 (2): 233-244.

Hinze, J.O. 1975. Experimental investigation on secondary currents in the turbulent flow through a straight conduit. *Appl. Sci. Res.*, 28: 453-465.

Labiod, C. and Masbernat, L. 2004. *Analyse paramétrique des lois de paroi en écoulement à surface libre sur fond de rugosité variable*. SIER, Laghouat, Algérie.

Launder, B.E., Reece, G.J. and Rodi, W. 1975. Progress in the development of a Reynolds-stress turbulence closure. *Journal of Fluid Mechanics*, 63 (3): 537-566.

Launder, B.E. and Li, S.-P. 1994. On the elimination of wall-topography parameters from second-moment closure. *Physics of Fluids*, 6(2): 999-1006.

Lund, E.G. 1977. *Mean flow and turbulence characteristics in the near corner region of square duct.* M.S. Thesis, Dept Mech. Engng, University of London.

Muller, A. and Studerus, X. 1979. Secondary flow in open channel. *Proceedings, Congress of International Associations for Hydraulic Research*, Italy, pp. 189-222.

Naimi, M. and Gessner, F. B. 1997. Calculation of fully-developed turbulent flow in rectangular ducts with non-uniform wall roughness. *Journal of Fluids Engineering, ASME,* 119 (9): 550-558.

Naot, D. and Rodi, W. 1982. Calculation of secondary currents in channel flows. *Journal of the Hydraulic Division, ASCE*, 108(8): 948-968.

Nezu, I. and Nakagawa, H. 1984. Cellular secondary currents in straight conduit. *Journal of Hydraulic Engineering, ASCE,* 110 (2): 173-193.

Nezu, I. and Rodi, .W. 1985. Experimental study on secondary currents in open channel flow. *21st IAHR Congress, Melbourne, Australia, pp.*115-119.

Nezu, I. and Rodi, W. 1986. Open-channel flow measurements with a laser Doppler anemometer. *Journal of Hydraulic Engineering, ASCE,* 112 (5): 335 –355.

Shir, C.C. 1973. A preliminary study of atmospheric turbulent flows in idealized planetary boundary layer. *Journal of Atmospheric Sciences*, 30: 1327-1339.

Spezial, C.G., Sarkar, S. and Gatski, T.B. 1991. Modelling the pressure-strain correlation of turbulence: an invariant dynamical systems approach. *Journal of Fluid Mechanics*, 227: 245-272.

Wang, Z.Q. and Cheng, N.S. 2006. Time-mean structure of secondary flows in open channel with longitudinal bed forms. *Adv. Water Resources*, pp. 1-16.

Zaouali, S. 2008. *Structure et modélisation d'écoulements à surface libre dans des canaux de rugosité inhomogène*. Thèse de l'INP de Toulouse.

Zaouali, S., Soualmia, A. and Masbernat, L. 2007. *Numerical simulation of an open channel flow with cross stream variation of the bottom roughness.* ISEH-V, Arizona.

Zeman, O. and Lumley, J.L. 1976. Modelling buoyancy-driven mixed layer. *Journal. Atmos. Sci.*, 33: 1974.